AgCuTi/graphene-reinforced Cu foam: A novel filler to braze ZrB_2-SiC ceramic to Inconel 600 alloy

Gang Wang[a,*], Yingjun Cai[a], Wei Wang[b], Xinjie Liu[a], Rujie He[c,*], Lu Zhang, Rongmei Liu [a], Caiwang Tan[d], Wei Cao[e,a]

a *Anhui Key Laboratory of High-performance Non-ferrous Metal Materials, Anhui Polytechnic University, Wuhu 241000, PR China*

b *School of Aviation and Materials, Anhui Machine and Electricity College, Wuhu 241002, PR China*

c I*nstitute of Advanced Structure Technology, Beijing Institute of Technology, Beijing 100081, PR China*

d *State Key Laboratory of Advanced Welding and Joining, Harbin Institute of Technology, Harbin 150001, PR China*

e *Nano and Molecular Systems Research Unit, University of Oulu, P.O. Box 3000, FIN-90014, Oulu, Finland*

Correspondence: herujie@bit.edu.cn; gangwang@ahpu.edu.cn

Abstract

In order to relieve high residual stresses between ceramics and metals during brazing processes, an AgCuTi/graphene-reinforced Cu foam composite filler was developed and used to braze the ZrB_2-SiC ceramic and Inconel 600 alloy. Microstructures and shear strengths of the joints were systematically studied. The joints are composed of $TiFe_2$, TiCu, TiC, Cu(s, s), Ag(s, s), and Ti_5Si_3 phases. It is found the addition of graphene on the Cu foam surface can effectively retard diffusions of metal atoms and avoid the collapse of the foam matrix. After being brazed at 900 ^oC, the joint can get a maximum shear strength of 157 MPa, much higher than those brazed without graphene addition. The high shear strength was investigated in detail and attributed to the integrity of the Cu foam, formation of the TiC and thickness of the reaction layer at the ceramic side.

Introduction

As one of the most important functional material groups, the advanced ceramics is fundamentally interesting due to complicated bonding mechanisms, and industrially important thanks to its unique high-temperature applications in the aerospace, electronics, and precision machinery areas [1,2]. However, these high-performance compounds suffer from inherent brittleness and poor machinability. Consequentially, it is hard to prepare them in large and complex shapes. To overcome this drawback, the self-joining of ceramics or connection to metals has been proposed. Up to date, joining ceramics and metals can be realized through brazing [3,4], diffusion bonding [5, 6], and transient liquid phase bonding [7,8]. However, unwanted residual stresses at joint interfaces turn out during the cooling processes because of poor wettability of ceramics and mismatches of coefficients of thermal expansion (CTE) between ceramics and metals. As a result, the overall joint quality is ruined. Thus, reductions of the residual stresses become critical to reach good joints.

Various efforts have been dedicated to relieving residual stresses. It is reported that the stresses can be relieved by using soft metallic interlayers [9,10], adding low CTE materials into fillers [11,12], fibers [13,14], particles [15,16] and using foam metals as interlayers [17-20]. Despites these progresses, poor distribution of fibers or particles yields uncontrollable reinforcements. Following the introduction of soft metallic interlayers, a detrimental interface is generated, and then accelerates the formation and expansion of cracks. Regarding residual stress reliefs, the use of metal foam is considered as an effective alternative to other methods. As a low CTE carbon

material, graphene has attracted considerable attentions due to its high mechanical properties, specific surface area, and low density [21, 22]. Up to now, graphene has been introduced into many alloy systems to obtain composite materials and improve mechanical properties of alloy. It also brings structural reinforcements as a filler [23-27]. Liu *et al.* reported add-on benefits of graphene nanosheets to the properties of a SnAgCu solder alloy. The wettability of the composite solders was also improved with the addition of graphene nanosheets [23]. A graphene/Cu composite interlayer was developed via CVD to braze the 6061 aluminum alloy. Results showed that graphene could effectively retard the element diffusions and hinder the intensive Al-Cu eutectic reaction [27]. However, it is noticed that graphene, subjected to the effect of van der Waals forces, is easily agglomerated if directly added into alloys [28]. Therefore, it is necessary to design a new composite interlayer which degrades graphene's aggregation.

The graphene-metal foam composite interlayer was recently proposed as an advanced type of fillers. Reinforced by graphene nanoplatelets, an AgCuTi composite filler was employed to braze the SiC ceramic and resulted in a higher strength than those without graphene contents [29]. A novel type of graphene reinforced Cu foam was exploited to braze the C/C composite and Nb. Graphene facilitated the retarding of metal atom diffusions and inhibited the collapse of the Cu foam [30]. A composite of graphene nanoplatelets reinforced TiCuZrNi was invented and applied to braze the C/C and Ti6Al4V. The shear strength was substantially improved thanks to the newly-formed TiC particles and existence of graphene nanoplatelets [31].

In the present work, the graphene reinforced Cu foam (G-Cu foam) has been developed and used as an interlayer to alleviate aggregation of graphene and relieve residual stresses at the joints between the ZrB_2-SiC ceramics (named as ZS) and Inconel 600 (named as In 600). The Cu foam was taken as a loading matrix thanks to its homogeneous distribution and persisting porous structure in the brazing seam according to our previous studies [32]. We systematically studied the impacts of the G-Cu foam interlayer on microstructural and mechanical properties at the ZS/In 600 joining parts. It is found that the graphene additive brings simultaneous benefits to the structural reinforcements and strengths.

Experimental

The ZS ceramic used in this work was prepared by a hot press sintering, provided by Center of Composite Materials of Harbin Institute of Technology. Details of the ZS preparation have been reported in Refs [20,33]. A nominal composition of In 600 alloy was Ni-15.5Cr-8Fe-1Mn-0.5Cu-0.5Si-0.1C (wt. %). Graphene oxide in the present work was synthesized by a modified Hummer's method [34, 35]. Briefly, 1.008 g graphite powder and 0.520 g $NaNO_3$ were added to the concentrated H_2SO_4 (23 mL) which was cooled to 0 °C in advance. After one hour, 3.002 g $KMnO_4$ was slowly added to carry out the reaction. Then, the mixture was stirred 30 min at 38 °C. After adding 80 mL water, the stirring was continued for another 30 min. Later, 200 mL water and 30% H_2O_2 (5.6 mL) were added in turn. After another 15 min stirring, the suspension was washed with HCl (37 %) to remove metal ions. Finally, the suspension was centrifuged at 2500 r/min. The supernatant was decanted, and then

washed with water several times until the product was neutral. The product was obtained after drying at 60 °C. 100 mg of the obtained graphene was slowly milled and mixed with isopropanol to get a slurry, which was coated on the Cu-foam. Finally, a G-Cu foam was obtained after being dried 12 hours at 60 °C.

The quality of G-Cu foams was assessed before brazing. Figures 1a and 1b depict microscopic images G-Cu foam. The average pore size is about 400 μm. Figure 1c shows a typical SEM image of graphene. Obvious wrinkles are found as marked by arrows, as the typical morphological feature of graphene [36,37]. Fig. 1d shows a Raman spectrum of the G-Cu foam used in this work. Two peaks at 1350 and 1590 cm^{-1} are observed, and attributed to the D and G bands of the in-plane sp^2 vibrations of C atoms, respectively [38,39]. The results agree well to the reported studies on the preparation of graphene [40-42].

ZS and In 600 were cut into dimensions of 4mm×4mm×4mm and 10 mm×10mm×4mm, respectively. The wire electrical discharge machining was used. Depending on equipment requirements, samples used for microstructural determinations and shear strength testing were formed into different sizes of 4 mm×4 mm×4 mm (ZS)/4 mm×4 mm×4 mm (In 600) and 4 mm×4 mm×4 mm (ZS)/10 mm×10 mm×4 mm (In 600). Fig. 1e shows a schematic diagram of the brazing assembly. The thicknesses of AgCu filler metal and Cu foam are 100 μm and 1 mm, respectively.

Prior to the brazing, the ZS and In 600 were carefully grounded and polished to reach flat surfaces. All materials were ultrasonically cleaned in alcohol for 10 min.

The brazing experiments were performed at 900 °C for 5 min, 15 min and 25 min, respectively. The microstructural determinations were carried on a scanning electron microscope (SEM, SU-8010) equipped with an energy-dispersive X-ray spectrometer (EDS). Shear testing was measured under an Instron 5500 testing machine. An average strength was obtained from measurements of three samples with the same brazing parameters.

Results and discussion

Figure 2 demonstrates typical microstructures and EDS results of the brazed joint of the ZS/AgCuTi/G-Cu foam/AgCuTi/In 600 alloy at 900 ^{o}C for 5 min. The joint is well connected. No obvious defects are detected in the joint. Element diffusion is sufficient, and reaction is accomplished, as shown in Fig.1a. Figures 1b to 1i depict element distributions in the joint. From the figures, the Ag and Cu from the filler are extensively distributed in the middle of the joint. The Ti from the filler and C from the graphene are also detected at the middle of the joint. They are prone to form the TiC. The Zr, Cr and Fe elements from the base materials mainly locate at the ZS side and In 600 side, respectively. It is worth noting that nickel from the In 600 alloy is also distributed in the whole joint due to chemical compatibility and physical solubility between the Cu and Ni.

Figure 3a shows a typical microstructure of ZS/AgCuTi/G-Cu foam/AgCuTi/In 600 joint brazed at 900 ^{o}C for 15 min. In the overview, the joint is about 400 μm width without defects. Moreover, three reaction zones are clearly distinguished in Fig.3a. They are the zone adjacent to In 600 alloy side, the brazing seam, and the zone

adjacent to ZS side. The brazing seam contains many discontinuous blocky gray structures, black phase (as marked by red arrows), and eutectic structure. The analyzed chemical compositions of different phases marked as A-H are listed in Table 1. Phase A with the blocky gray structures is identified as the Cu(s, s), consistent with the previous result where the Cu foam was employed as an interlayer [20]. These blocks Cu(s, s) mainly originates from the Cu foam. The black phase B contains Ti and C at an approximate atomic ratio of 1:1, and thus is inferred as the TiC phase from the reaction of Ti + C → TiC. Fig. 3b is the enlarged images of reaction layer at In 600 side. Based on contrast, three phases marked as C to E are shown. According to the content of elements, the black strip-like phase C is $TiFe_2$. It was reported that the Fe showed a strong tendency to react with the Ti. A product of $TiFe_2$ was resulted from the reaction of $Fe + 2Ti \rightarrow TiFe_2$ [43]. In fact, the $TiFe_2$ is easily formed as soon as the Fe dissolve from the In 600 alloy into the liquid AgCuTi filler. The element of phase D is mainly silver. Thus, phases D is inferred as Ag(s, s). Phase E has an Ti/Cu atomic ratio of 1:1, and can be considered as the TiCu phase according to the Ti-Cu binary diagram [44]. At 900 ^{o}C, the main reaction between the Ti and Cu underwent the processes of Ti +Cu = TiCu (ΔG = -17069 + 4.887 T = -11336.549 J/mol) [45]. Due to the low Gibbs free energy, the TiCu occupied a large proportion in the reaction layer at the In 600 side. Fig. 3c displays the zoomed image of eutectic structure from Fig.3a. Moreover, based on the EDS results, the F and G phases are considered as Cu(s, s) and Ag(s, s), respectively. Combined with the result of Fig. 3a, the Ag-Cu eutectic structure occupied half areas of the brazing seam, which is the typical feature

of brazing by AgCu-based filler [46,47]. Fig. 3d demonstrates the zoomed image at the ZS side. Many Cu(s,s) and AgCu eutectic structure can also be found. The Ti, C and Si elements are the main composites according to EDS of phase H. The Ti can easily react with the SiC to form TiC and Ti_5Si_3 phases based on the reaction of Ti + SiC→Ti_5Si_3 + TiC. From the above analysis, the In 600/AgCuTi/G-Cu foam/AgCuTi/ ZS brazed joint is composed of In 600/Ag(s, s) + $TiFe_2$ + TiCu/ Ag(s, s) + Cu(s, s) + TiC/Ti_5Si_3 + TiC/ZS ceramic.

Table 1 Chemical compositions of each phases as marked in Fig.3

	Ag	Cu	Ti	C	Ni	Cr	Fe	B	Si	Zr	phase
A	2.07	83.18	2.58	7.31	1.08	0.92	1.26	1.33	0.27	-	Cu(s,s)
B	1.52	1.52	46.26	41.32	0.77	0.58	0.83	3.46	0.53	0.02	TiC
C	0.14	8.81	28.57	1.13	9.65	6.07	45.20	0.49	0.91	0.02	$TiFe_2$
D	79.01	6.40	2.68	1.90	1.79	3.04	1.86	1.97	0.90	0.44	Ag(s,s)
E	0.39	35.40	29.57	17.10	3.08	1.02	12.08	0.63	0.68	0.05	TiCu
F	2.74	80.45	3.31	6.40	2.09	1.15	1.57	1.34	0.85	0.13	Cu(s,s)
G	76.52	8.40	0.78	3.13	2.45	2.17	3.18	1.21	2.03	0.13	Ag(s,s)
H	1.83	6.91	40.05	25.52	3.37	0.97	5.54	6.28	9.38	0.16	Ti_5Si_3+TiC

The brazing time influences on joint microstructures were investigated. Fig. 4 depicts the microscopies of the joint brazed with the G-Cu foam at 900 ^oC but with different time. For brazing time of 5 min and 15 min (Fig. 4a and 4b), plenty Cu(s, s) blocks and Ag-Cu eutectic structures remained and homogeneously distributed in the entire brazing seam. This serves a direct approval of the preservation of the G-Cu frame structure in the joint. Thanks to its uniform dispersion, the Cu(s,s) can greatly release the thermal residual stresses and accommodate strains by its plastic deformation. As a result, the joints are strengthened [48]. However, the seam possesses unhomogeneously distributed Cu(s, s) after being brazed 25 minutes, as shown in Fig. 4c. The G-Cu foam collapsed, decreasing residual stress reliefs. The

thickness of reaction layer in ZS side increased from 1.1 μm to 4.6 μm when the brazing time increased from 5 min to 25 min, as indicated in Fig. 4d to 4f. At a short brazing time of 5 min the reaction layer might not be thick enough to form a reliable metallic bonding. Moreover, cracks appeared on the interface when brazing time was 25 min, as shown in Fig. 4f, which was harmful to the properties of joint.

Shear strengths were plotted in Fig.5 for the joints brazed at 900 ^{o}C but different in time with the G-Cu foam as the filler. Overall, the shear strength exceeds 100 MPa, higher than the one only using the bare Cu foam as the interlayer [32]. The shear strengths are 138 MPa, 157 MPa and 102 MPa, respectively, for the brazing time of 5 min, 15 min and 25 min. This demonstrates that the introduction of graphene on the form can strengthen the joints. The mechanism leading to strength enhancements can be explained as follows. In general, graphene is a two-dimension carbon layer with a sp^2 hybridization and has higher bond energy than other carbon forms. A strong energy barrier is set by the chemical stability of the graphene when reacting with metals. Up to now, many researchers have used graphene for preventing the reaction or inter-diffusion at the interfaces of Al/Si, Au/Ni, Cu/Si and so on [49-51]. Kim *et al.* demonstrated an effective obstruction of reactions between the Al and Si and the intermixing of Au and Ni at high temperatures using graphene as a barrier [49]. Hong *et al*. reported the use of thin graphene layers as a diffusion barrier during the Cu metallization at high temperature regimes of 500-900 ^{o}C. The addition of graphene effectively blocked diffusions of Cu atoms into the Si [50]. Nguyen *et al*. also used 1 nm thick graphene as a Cu diffusion barrier. Therein graphene was thermally stable

against Cu diffusion and no inter-diffusion in the Cu/graphene structure took place [51]. The outstanding performance of graphene as a metal diffusion prohibitor is very useful to improve the stability of the metallizations. In addition, it is reported that the size of intrinsic “pore” of hexagonal lattice in graphene is about 0.064 nm, which is much smaller than atomic radius of the main elements in the present work, i.e. Ag 0.134 nm, Cu 0.117 nm and Ti 0.132 nm. This difference in size also makes it difficult for metal atoms to pass through graphene [52,53]. Furthermore, the solid solubility of C in Cu at high temperature is rather small, e.g., ranging from 4.8 ± 0.5 ppm at 1143 K to 7.4 ± 0.5 ppm at 1293 K [54]. Based on the above studies, for the present work, graphene reinforced in Cu foam can block the diffusion of the Cu atom, and protect the structural integrity of the Cu foam, making it less probable to collapse. At the matrix side, the Cu foam with a good structural integrity helps to relieve the residual stress of the joint, leading to a higher shear strength compared to cases in the absence of graphene during the brazing (Fig.5). As shown in Figs.5a-c, the TiC phases were detected in the brazing seam, and subjected to two main reaction paths. In the first one, the Ti atoms from the filler react with the C atoms diffused from the ZS ceramics to form TiC due to the large negative Gibbs free energy [55]. In the second, though not reacting with Cu, graphene shows good affinity with Ti, and is easy to form Ti-C compounds. It is reported that metals like Pd and Ti readily react with graphitic carbons, resulting in Pd- and Ti-carbides [56]. Due to a rather simple but facile preparation process in the present work, defects in graphene are inevitable. The Ti can easily react with the defected graphene to form a TiC phase. The formation and

evenly distribution of TiC in the brazing seam is beneficial to strengthen the joints due to its positive effect on refinement of the crystal-microstructure of brazed fillers [57]. Furthermore, the CTE discrepancy between the TiC ($6.52 \times 10^{-6}\,K^{-1}$ [58]) and ZS ($4.0\times 10^{-6}\,K^{-1}$ [20]) is smaller than that between the AgCuTi brazing filler ($18.2 \times 10^{-6}\,K^{-1}$ [58]) and the ceramics. The CTE mismatch is substantially reduced. These combined effects facilitate the joint strength enhancement.

We also noticed after 25 min brazing, the value of shear strength became lower than those after 5 min and 10 min brazing. The strength decrease can be explained as follows. With prolongation of the holding time, the softening problem of Cu foam was more pronounced, and some areas collapsed, thus forming a large area of Cu-based solid solution, as shown in Fig. 4c. This is destructive to the maintenance of high shear strength joints. Furthermore, increasing the brazing time can result in the formation of larger amount of TiC and Ti_5Si_3 brittle intermetallics in the interface. The existence of these thicker brittle intermetallics impairs with the plastic deformation of the joint, which is harmful to the relaxation of residual stress in the joint. In fact, the observed micro-cracks in Fig.4f was resulted from the residual stress concentration in the interface but lead to the mechanical property deteriorations [59].

The schematic of the strengthening role of the G-Cu foam composite interlayer in the joint seam is depicted in Fig. 6. Fig.6a shows the cross section of the assembly of the brazing joint. The G-Cu form composite interlayer was prepared and installed in the middle of joint. Graphene was evenly distributed on the surface of Cu foam due to its inner-connective porosity. When heated to the melting point of filler, the molten

AgCuTi filler flowed and wetted the In 600 and ZS. At the ZS side, a reaction between Ti and Si (Ti + Si → Ti_5Si_3) occurred due to its lowest Gibbs free energy among related peers. Meanwhile, the TiC was also produced through the path of Ti + C → TiC [60]. At the In 600 side, the $TiFe_2$ from the reaction of Fe + 2Ti→$TiFe_2$ was formed due to a strong reaction tendency between the Fe and Ti, as shown in Fig.6b. During this process, the molten AgCuTi filler metal partially began to fill the G-Cu foam. With further heating to the brazing temperature, the G-Cu foam began to be soften and pressed. An Ag-Cu eutectic structure consisting of Ag(s,s) and Cu(s,s) was formed in the brazing seam, which is consistent with results reported in Refs [11,61,62]. The Ti in the filler reacted with the Cu, forming a TiCu phase via Ti + Cu → TiCu reaction, as shown in Fig.6c. The rest Ti, Ag and Cu elements continuously reacted with the G-Cu foam. Especially for the Ti, it was adsorbed on the defective places at the surface of G-Cu foam. These defects could consume the Ti to form a TiC phase, as shown in Fig.6d. However, during this process, the frame structure of Cu foam was kept. Fig.6e demonstrates the joint microstructure after the brazing. The Cu(s, s) and TiC were homogeneously distributed in the entire joint seam. The homogeneously distributed Cu(s, s) owns a good plastic deformation capacity that brings effective reliefs of residual stresses. The TiC particles act as a reinforcement phase in the joint, and benefit the joint strength.

Conclusion

In summary, a sound joint between the ZS ceramic and In 600 alloy was achieved using the AgCuTi/G-Cu foam composite filler and being brazed at 900 ^{o}C.

The typically interfacial microstructures of the brazed joint were In 600 alloy/$TiFe_2$/TiCu/TiC/Cu(s,s) +Ag(s,s)/TiC+Ti_5Si_3/ZS ceramic. All brazed joint possessed high shear strengths above 100 MPa, higher than the joint brazed using the AgCuTi with sole Cu foam. The existence of graphene on the surface of the Cu foam can effectively hinder diffusions of Cu atoms and protect the form's structural integrity, resulting in the homogeneous distribution of Cu(s, s) in the brazing seam and consequently relieving residual stresses. Meanwhile, the formation of TiC phase in the joint also played a positive role of strength reinforcements. The above combined effects can remarkably improve the shear strength at the joint.

Acknowledgement

This work was financially supported by the National Natural Science Foundation of China [51704001]; Talent Project of Anhui Province [Z175050020001]; Natural Science Foundation of Anhui Province [KJ2018A0860], Talent Project of Anhui Polytechnic University, Anhui Provincial Grant for high-level platform construction, and the Academy of Finland [No. 311934].

References

1. F. Aldinger, V.A. Weberruss, Advanced ceramics and future materials: An introduction to structures, properties, technologies, methods; Vch-Pub, Germany, 2010, 170-260.
2. S. Simões, Recent progress in the joining of Titanium alloys to ceramics, Metals. 8(2018) 876.
3. F. Valenza, C. Artini, A. Passerone, P. Cirillo, M.L. Muolo, Joining of ZrB_2 ceramics to Ti6Al4V by Ni-based interlayers. J. Mater. Eng. Perform. 23 (2014) 1555-1560.
4. J.M. Shi, L.X. Zhang, X.Y. Pan, X.Y. Tian, J.C. Feng, Microstructure evolution and mechanical property of ZrC-SiC/Ti6Al4V joints brazed using Ti-15Cu-15Ni filler. J. Eur. Ceram. Soc. 38 (2018) 1237-1245.

5. M.I. Barrena, L. Matesanz, J.M. Gómez de Salazar, Al_2O_3/Ti6Al4V diffusion bonding joints using Ag-Cu interlayer. Mater. Charact. 60 (2009) 1263-1267.
6. X. Yu, H. Zhao, Z. Huang, X. Chen, Y. Aman, S. Li, H. Zhai, Z. Guo, S. Xiong, Microstructure evolution and bonding mechanism of Ti2SnC-Ti6Al4V joint by using Cu pure foil interlayer. Mater. Charact. 127 (2017) 53-59.
7. J.D. Sugar, J.T. Mckeown, T. Akashi, S.M. Hong, K. Nakashima, A.M. Glaeser, Transient-liquid-phase and liquid-film-assisted joining of ceramics. J. Eur. Ceram. Soc. 26(2006)363-372.
8. J. Lemus-Ruiz, A.O. Guevara-Laureano, J. Zarate-Medina, A. Arellano-Lara, L. Ceja-Cárdenas, Interface behavior of Al_2O_3/Ti joints produced by liquid state bonding. Appl. Radiat. Isot. 98(2015) 1-6.
9. J.C. Feng, D. Liu, L.X. Zhang, X.C. Lin, P. He, Effects of processing parameters on microstructure and mechanical behavior of SiO_2/Ti-6Al-4V joint brazed with AgCu/Ni interlayer, Mater. Sci. Eng. A 527 (2010) 1522-1528.
10. Z.W. Yang, L.X. Zhang, Y.C. Chen, J.L. Qi, P. He, J.C. Feng, Interlayer design to control interfacial microstructure and improve mechanical properties of active brazed Invar/SiO_2-BN joint, Mater. Sci. Eng. A 575 (2013) 199-205.
11. B. Cui, J.H. Huang, J.H. Xiong, H. Zhang, Reaction-composite brazing of carbon fiber reinforced SiC composite and TC4 alloy using Ag-Cu-Ti-(Ti + C) mixed powder, Mater. Sci. Eng. A 562 (2013) 203-210.
12. H. Chen, J. Peng, L. Fu, Effects of interfacial reaction and atomic diffusion on the mechanical property of Ti_3SiC_2 ceramic to Cu brazing joints, Vacuum. 130 (2016) 56-62.
13. G.B. Lin, J.H. Huang, H. Zhang, Joints of carbon fiber-reinforced SiC composites to Ti-alloy brazed by Ag-Cu-Ti short carbon fibers, J. Mater. Process. Technol. 189 (2007) 256-261.
14. D.Y. Fan, J.H. Huang, Y.H. Wang, S.H. Chen, X.K. Zhao, Active brazing of carbon fiber reinforced SiC composite and 304 stainless steel with Ti-Zr-Be, Mater. Sci. Eng. A 617 (2014) 66-72.
15. X. Wang, L.F. Cheng, S.W. Fan, L.T. Zhang, Microstructure and mechanical properties of the GH783/2.5DC/SiC joints brazed with Cu-Ti+Mo composite filler, Mater. Des. 36 (2012) 499-504.
16. Q. Qiu, Y. Wang, Z. Yang, X. Hu, D. Wang, Microstructure and mechanical properties of TiAl alloy joint vacuum brazed with Ti-Zr-Ni-Cu brazing powder without and with Mo additive, Mater. Des. 90 (2016) 650-659.
17. A. Junga, J. Luksch, S. Diebels, F. Schäfer, C. Motz, In-situ and ex-situ microtensile testing of individual struts of Al foams and Ni/Al hybrid foams, Mater. Des. 153 (2018) 104-119.
18. M.N. Feng, Y. Xie, C.F. Zhao, Z. Luo, Microstructure and mechanical performance of ultrasonic spot welded open cell Cu foam/Al joint, J. Manuf. Process. 33 (2018) 86-95.
19. T. Zaharinie, R. Moshwan, F. Yusof, M. Hamdi, T. Ariga, Vacuum brazing of sapphire with Inconel 600 using Cu/Ni porous composite interlayer for gas pressure sensor application, Mater. Des. 54 (2014) 375-381.

20. G. Wang, Z.T. Wang, W. Wang, R.J. He, K.X. Gui, C.W. Tan, W. Cao. Microstructure and shear strength of ZrB_2-SiC/Ti-6Al-4V joint by TiCuZrNi with Cu foam. Ceram. Int. 45 (2019) 10223-10229
21. S. Stankovich, D.A. Dikin, G.H.B. Dommett, K.M. Kohlhaas, E. Zimney, E.A. Stach,R.D. Piner, S.T. Nguyen, R.S. Ruoff, Graphene-based composite materials, Nature. 442 (2006) 282-286.
22. W.J. Kim, T.J. Lee, S.H. Han, Multi-layer graphene/copper composites: preparation using high-ratio differential speed rolling, microstructure and mechanical properties, Carbon 69 (2014) 55-65.
23. X. Liu, Y. Han, H. Jing, J. Wei, L. Xu, Effect of graphene nanosheets reinforcement on the performance of Sn-Ag-Cu lead-free solder, Mat. Sci. Eng. A. 562 (2013)25-32.
24. L.Y. Xu, Z.K. Zhang, H.Y. Jing, J. Wei, Y.D. Han, Effect of graphene nanosheets on the corrosion behavior of Sn-Ag-Cu solders, J. Mater. Sci: Mater. Electron. 26 (2015) 5625-5634.
25. Y. Huang, Z. Xiu, G. Wu, Y. Tian, P. He, Sn-3.0Ag-0.5Cu nanocomposite solders reinforced by graphene nanosheets, J. Mater. Sci: Mater. Electron. 27 (2016) 6809-6815.
26. S. Li, Y. Liu, H. Zhang. Microstructure and hardness of SAC305 and SAC305-0.3 Ni solder on Cu, high temperature treated Cu, and graphene-coated Cu substrates. Results. Phys, 11(2018) 617-622.
27. J.L. Qi, Z.Y.Wang, J.H. Lin, T.Q. Zhang, A.T. Zhang, J. Cao, L.X. Zhang, J.C. Feng. Graphene-enhanced Cu composite interlayer for contact reaction brazing aluminum alloy 6061. Vacuum. 136 (2017) 142-145.
28. F. Chen, J. Ying, Y. Wang, S. Du, Z. Liu, Q. Huang, Effects of graphene content on the microstructure and properties of copper matrix composites, Carbon 96 (2016) 836-842.
29. Y.Y. Song, D. Liu, S.P. Hu, X.G. Song, J. Cao. Graphene nanoplatelets reinforced AgCuTi composite filler for brazing SiC ceramic. J. Eur. Ceram. Soc. 39 (2019) 696-704.
30. Z.Y. Wang, G. Wang, M.N. Li, J.H. Lin, Q. Ma, A.T. Zhang, Z.X. Zhong, J.L. Qi, J.C. Feng. Three-dimensional graphene-reinforced Cu foam interlayer for brazing C/C composites and Nb. Carbon 118 (2017) 723-730.
31. X.R. Song, H.J. Li, X.R. Zeng, L.L. Zhang. Brazing of C/C composites to Ti6Al4V using graphene nanoplatelets reinforced TiCuZrNi brazing alloy. Mater. Lett. 183 (2016)232-235.
32. G. Wang, Y.J. Cai, W.Wang, K.X. Gui, D.D. Zhu, C.W. Tan, W. Cao. Brazing ZrB_2-SiC ceramics to Inconel 600 alloy without and with Cu foam. J. Manuf. Process. 41 (2019) 29-35.
33. X.H. Zhang, P. Hu, J.C. Han, Structure evolution of ZrB_2-SiC during the oxidation in air, J. Mater. Res. 23 (2008) 1961-1972.
34. W.S. Hummers, R.E. Offeman, Preparation of graphitic oxid*e.* J. Am. Chem. Soc., 80 (1958) 1339.
35. Y.X. Xu, H. Bai, G.W. Lu, C. Li, G.Q. Shi. Flexible graphene films via the

filtration of water-soluble noncovalent functionalized graphene sheets. J. Am. Chem. Soc., 130 (2008) 5856-5857.
36. M. Wang, L.D. Wang, J. Sheng, Z.Y. Yang, Z.D. Shi, Y.P. Zhu, J. Li, W.D. Fei. Direct synthesis of high-quality graphene on Cu powders from adsorption of small aromatic hydrocarbons: A route to high strength and electrical conductivity for graphene/Cu composite, J. Alloy. Compd. 798 (2019) 403-413
37. L.Y. Zhang, L. Zhang, J. Zhang, P. Xue, W.W. Hao, M. Shen, H.H. Zheng. In situ growth of three-dimensional graphene coatings on arbitrary-shaped micro/nano materials and its mechanism studies. Carbon 92 (2015) 84-95
38. Z.S. Xu, X.L. Shi, W.Z. Zhai, J. Yao, S.Y. Song, Q.X. Zhang, Preparation and tribological properties of TiAl matrix composites reinforced by multilayer graphene, Carbon 67 (2014) 168-177.
39. A. Eckmann, A. Felten, A. Mishcenko, L. Britnell, R. Krupke, K.S. Novoselov, et al., Probing the nature of defects in graphene by Raman spectroscopy, Nano. Lett. 12 (2012) 3925-3930.
40. J. Dutkiewicz, P. Ozga, W. Maziarz, J. Pstru_s, B. Kania, P. Bobrowski, J. Stolarska, Microstructure and properties of bulk copper matrix composites strengthened with various kinds of graphene nanoplatelets, Mater. Sci. Eng. A 628 (2015) 124-134.
41. M. Strankowski, D. WBodarczyk, A. Piszczyk, J. Strankowska, Polyurethane nanocomposites containing reduced graphene oxide, FTIR, Raman, and XRD studies, J. Spectrosc. 2016 (2016) 1-6.
42. L.X. Zhang, B. Zhang, Z. Sun, X.Y. Tian, M. Lei, J.C. Feng. Preparation of the graphene nanosheets reinforced AgCuTi based composite for brazing graphite and Cu, J. Alloy. Compd. 782 (2019) 981-985.
43. Z. Sun, L.X. Zhang, J.L. Qi, Z.H. Zhang, C.L. Tian, J.C. Feng. Brazing of SiO_{2f}/SiO_2 composite modified with few-layer graphene and Invar using AgCuTi alloy. Mater. Des. 88 (2015) 51–57
44. X. Dai, J. Cao, J. Liu, D. Wang, J. Feng, Interfacial reaction behavior and mechanical characterization of ZrO_2/TC4 joint brazed by Ag-Cu filler metal, Mater. Sci. Eng. A 646 (2015) 182-189.
45. Y.P. Liu, G. Wang, W. Cao, H.T. Xu, Z.J. Huang, D.D. Zhu, C.W. Tan. Brazing ZrB_2-SiC ceramics to Ti6Al4V alloy with TiCu-based amorphous filler. J. Manuf. Process. 30 (2017) 516-522
46. Q.W. Qiu, Y.Wang, Z.W. Yang, D.P. Wang. Microstructure and mechanical properties of Al_2O_3 ceramic and Ti6Al4V alloy joint brazed with inactive Ag-Cu and Ag-Cu + B. J. Eur. Ceram. Soc. 36(2016) 2067-2074.
47. L.M. Pan, J. Gu, W.J. Zou, T. Qiu, H.B. Zhang, J. Yang, Brazing joining of Ti3AlC2 ceramic and 40Cr steel based on Ag-Cu-Ti filler Metal. J. Mater. Process. Technol. 251(2018)181-187.
48. A.A. Shirzadi, Y. Zhu, H.K.D.H. Bhadeshia, Joining ceramics to metals using metallic foam, Mater. Sci. Eng. A 496 (2008) 501-506.
49. H. Kim, C. Lee, J. Kim, F. Ren, S. J. Pearton,Graphene as A Diffusion Barrier for Al and Ni/Au Contacts on Silicon. J. Vac. Sci. Technol. B 30 (2012)030602.

50. J. Hong, S. Lee, S. Lee, H. Han, C. Mahata, H. Yeon, B. Koo, S. Kim, T. Nam, K. Byun, Graphene as an Atomically Thin Barrier to Cu Diffusion into Si. Nanoscale 6 (2014)7503-7511.
51. B. Nguyen, J. Lin, D. Perng, 1-nm-Thick Graphene Tri-Layer as the Ultimate Copper Diffusion Barrier. Appl. Phys. Lett. 104(2014) 082105.
52. V. Berry, Impermeability of graphene and its applications, Carbon. 62 (10) (2013) 1-10.
53. Y.D. Zhao, Z.J. Liu, T.Y. Sun, L. Zhang, W.J. Jie, X.S. Wang, et al., Mass transport mechanism of Cu species at the metal/dielectric interfaces with a graphene barrier, ACS Nano 8 (2014) 12601-12611.
54. G.A. López, E.J. Mittemeijer, The solubility of C in solid Cu, Scr. Mater. 51(1) (2004) 1-5.
55. Y.H. Zhou, D. Liu, H.W. Niu, X.G. Song, X.D. Yang, J.C. Feng, Vacuum brazing of C/C composite to TC4 alloy using nano-Al2O3 strengthened Ag-Cu-Ti composite filler, Mater. Des. 93 (2015) 347-356.
56. C. Gong, S.M. Donnell, X.Y. Qin, A. Azcatl, H. Dong, Y.J. Chabal, et al., Realistic metal-graphene contact structures, ACS Nano 8(2013) 642-649.
57. Z.Y. Wang, M.N. Li, J. Ba, Q. Ma, Z.Q. Fan, J.H. Lin, Z.X. Zhong, J.L. Qi, J. Cao,J.C. Feng, In-Situ synthesized TiC nano-flakes reinforced C/C composite-Nb brazed joint, J. Eur. Ceram. Soc. 38 (2018) 1059-1068.
58. Q. Miao, W.F. Ding, Y.J. Zhu, Z.Z. Chen, Y.C. Fu, Brazing of CBN grains with Ag-Cu-Ti/TiX composite filler-the effect of TiX particles on microstructure and strength of bonding layer, Mater. Des. 98 (2016) 243-253.
59. X.Y. Tian, J.C. Feng, J.M. Shi, H.W. Li, L.X. Zhang, Brazing of ZrB_2-SiC-C ceramic and GH99 superalloy to form reticular seam with low residual stress. Ceram. Int. 41 (2015) 145-153.
60. T. Wang, B.G. Zhang, T. Yu, R.S. Li, X.P. Li, H.Q. Wang, Microstructural evolution mech-anisms of Ti600 and Ni-25%Si joint brazed with Ti-Zr-Ni-Cu amorphous filler foil. J. Mater. Process. Technol. 240 (2017) 414-419.
61. F. Valenza, C. Artini, A. Passerone, M.L. Muolo. ZrB_2–SiC/Ti6Al4V joints: wettability studies using Ag- and Cu-based braze alloys, J. Mater. Sci. 47 (2012) 8439-8449.
62. L.M. Pan, J. Gu, W.J. Zou, T. Qiu, H.B. Zhang, J. Yang. Brazing joining of Ti_3AlC_2 ceramic and 40Cr steel based on Ag-Cu-Ti filler Metal, J. Mater. Process. Technol. 251 (2018) 181-187.

Figure and Caption

Fig.1 a)–c) SEM images of G-Cu foam, d) Raman spectrum of G-Cu-foam and e) schematic diagram of brazing assembly

Fig 2 .a) Microstructure and b) to i) corresponding EDS results of brazed joint at 900 ^{o}C for 5 min

Fig.3 Typical microstructure of brazed joint at 900 ^{o}C for 15 min: a) whole morphology; b) enlarged image of In 600 side; c) enlarged image of eutectic structure and d) enlarged image of ZS side

Fig.4 Microstructure of joints brazed at 900 ^{o}C for different times: a), d) 5 min; b), e) 15 min and c), f) 25 min

Fig.5 Shear strength of joints brazed at 900 ^{o}C for different time using G-Cu foam

Fig.6 Schematic diagram of the formation of brazed joint

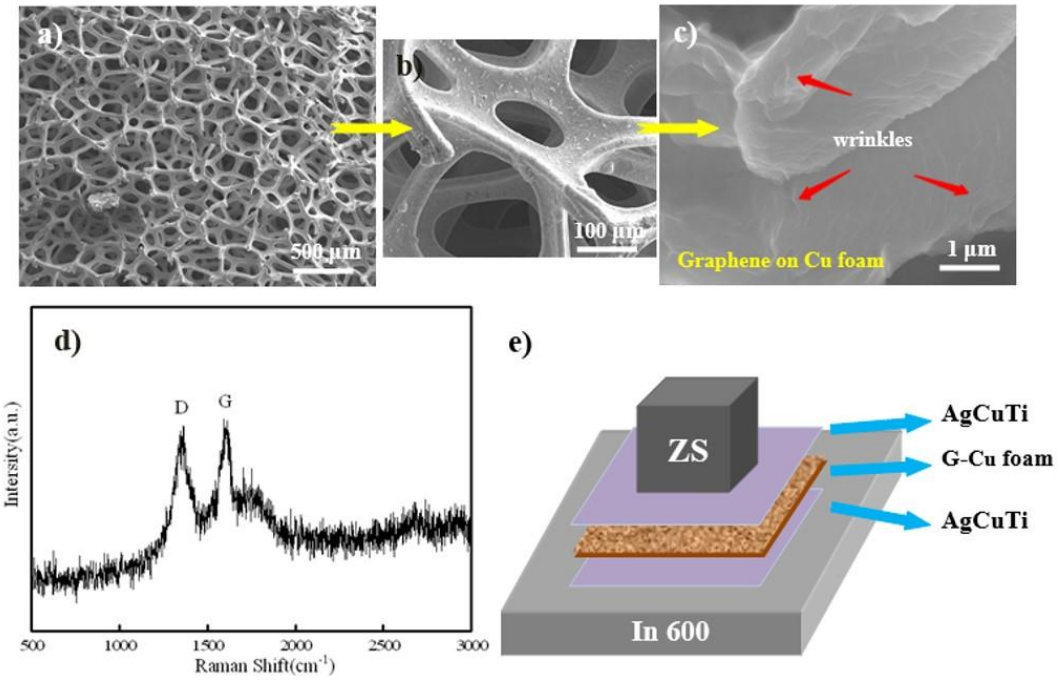
a)
500 μm
b)
100 μm
c)
wrinkles
Graphene on Cu foam
1 μm
d)
D
G
Intensity(a.u.)
500
1000
1500
2000
2500
3000
Raman Shift(cm-1)
e)
ZS
AgCuTi
G-Cu foam
AgCuTi
In 600

Fig.1

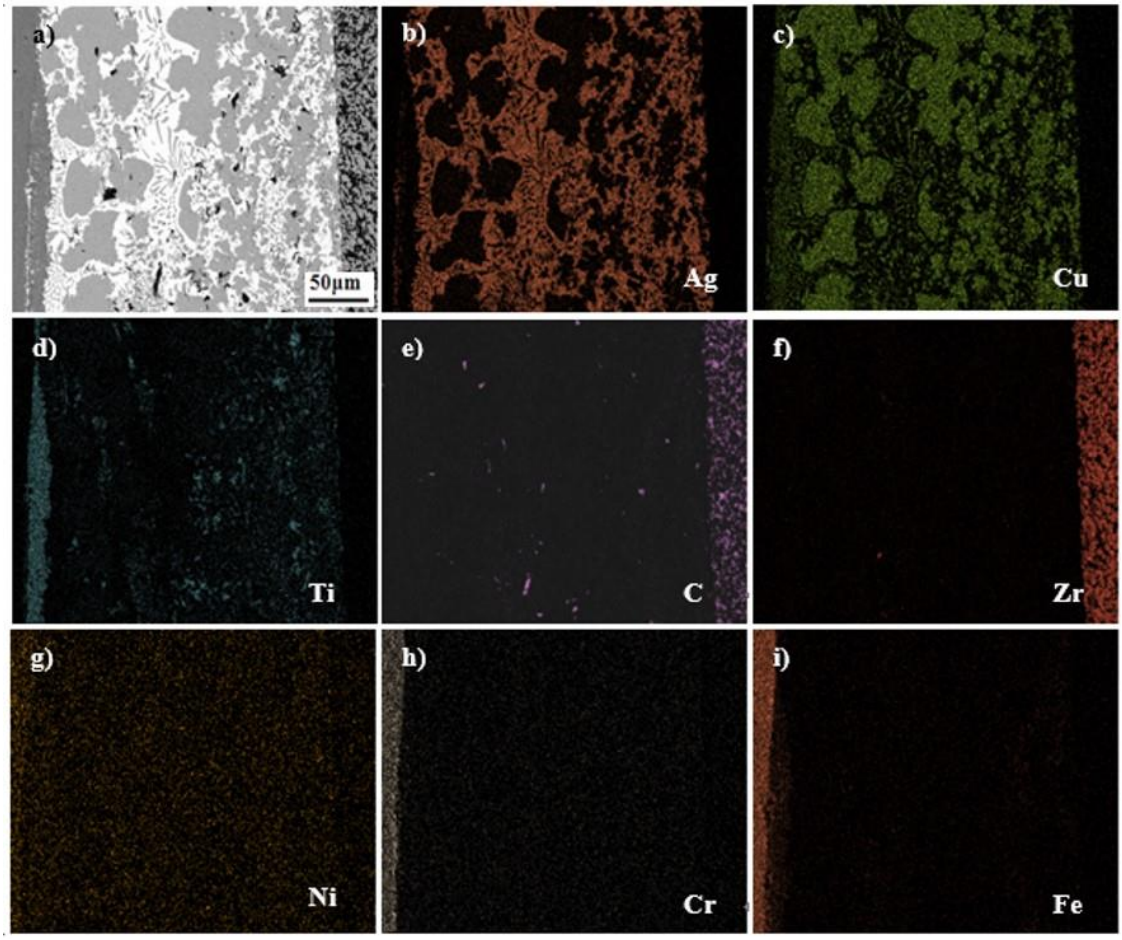
a)
50μm
b)
Ag
c)
Cu
d)
Ti
e)
C
f)
Zr
g)
Ni
h)
Cr
i)
Fe

Fig.2

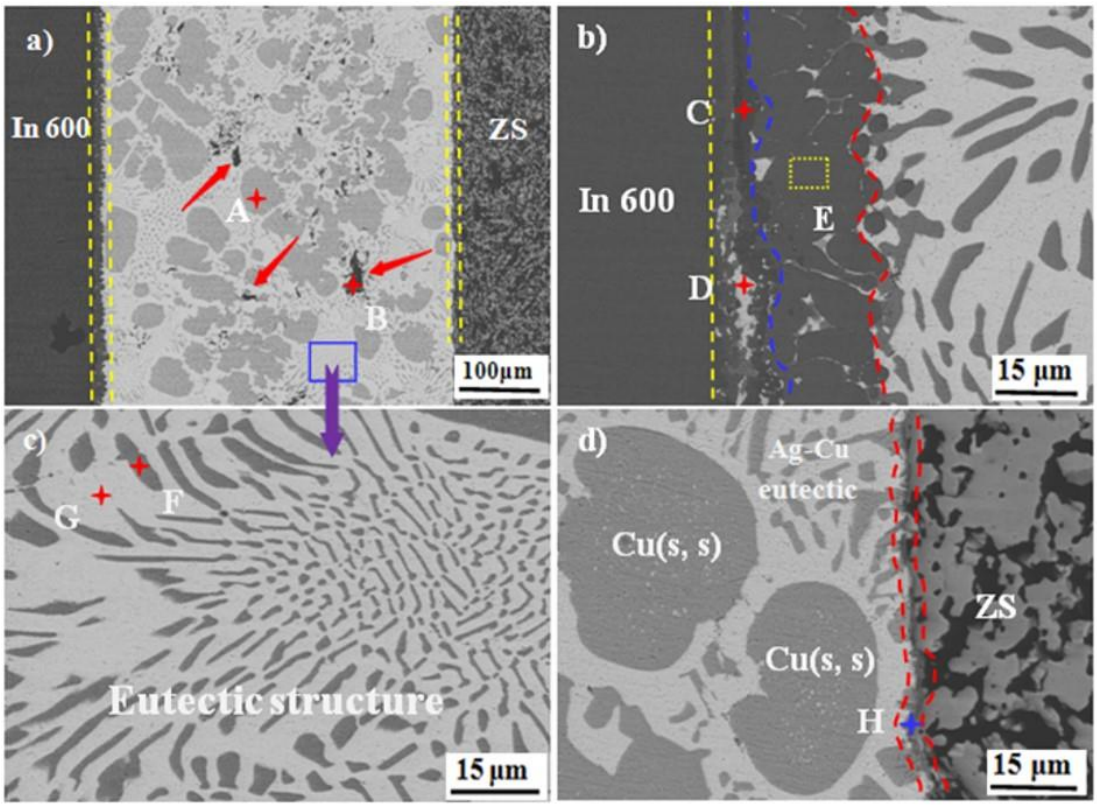
a)
In 600
ZS
A
B
100μm
b)
C
In 600
E
D
15 μm
c)
G
F
Eutectic structure
15 μm
d)
Ag-Cu
eutectic
Cu(s, s)
ZS
Cu(s, s)
H
15 μm

Fig.3

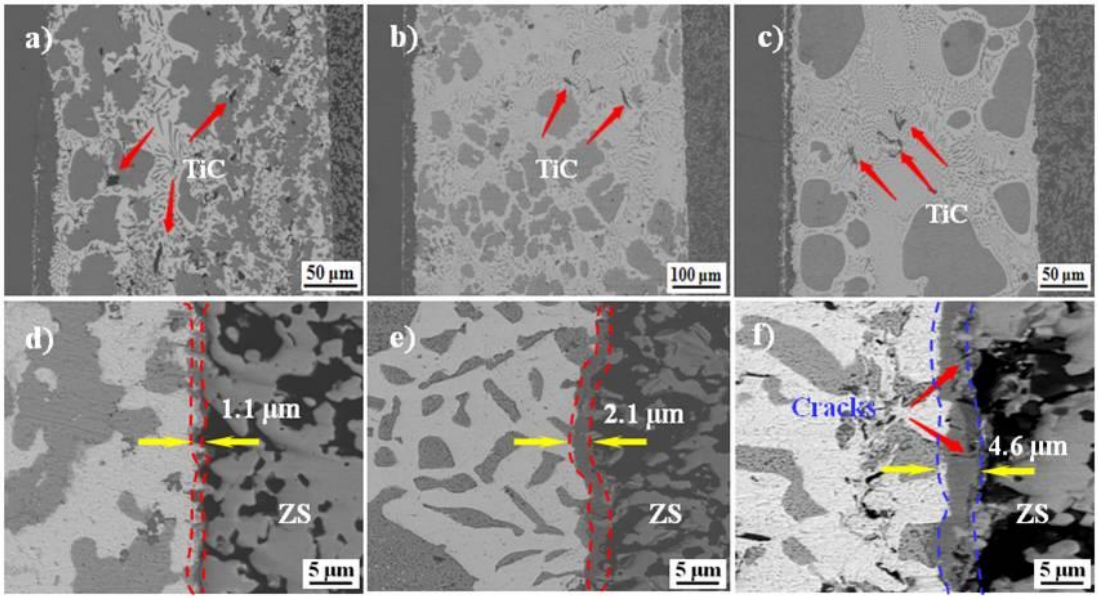
a)
TiC
50 μm
b)
TiC
100 μm
c)
TiC
50 μm
d)
1.1 μm
ZS
5 μm
e)
2.1 μm
ZS
5 μm
f)
Cracks
4.6 μm
ZS
5 μm

Fig.4

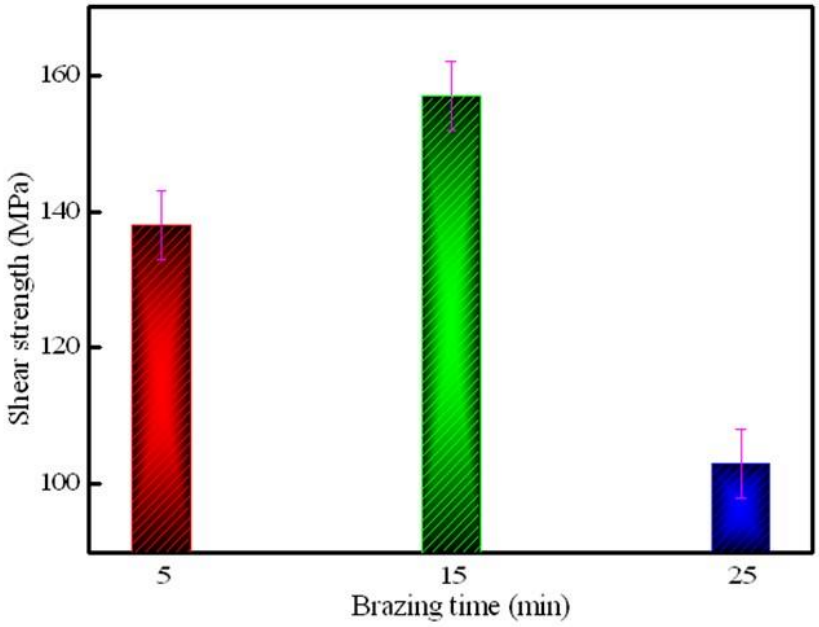
160
140
120
100
Shear strength (MPa)
5
15
25
Brazing time (min)

Fig.5

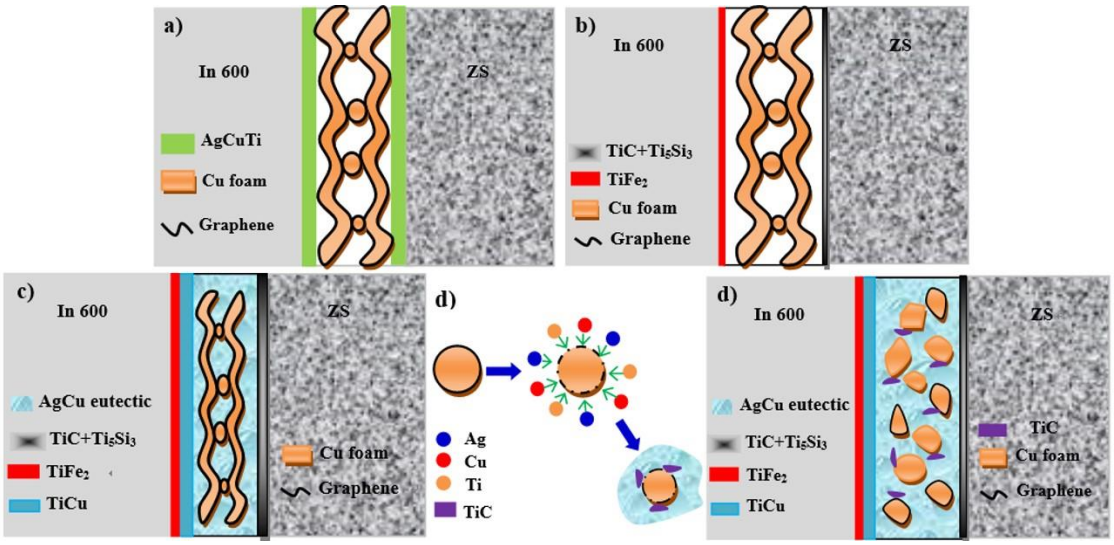
a)
In 600
ZS
AgCuTi
Cu foam
Graphene
b)
In 600
ZS
TiC+Ti5Si3
TiFe2
Cu foam
Graphene
c)
In 600
ZS
AgCu eutectic
TiC+Ti5Si3
TiFe2
TiCu
Cu foam
Graphene
d)
Ag
Cu
Ti
TiC
d)
In 600
ZS
AgCu eutectic
TiC+Ti5Si3
TiFe2
TiCu
TiC
Cu foam
Graphene

Fig.6